

Event plane resolution correction for azimuthal anisotropy in wide centrality bins

Hiroshi Masui and Alexander Schmah

Lawrence Berkeley National Laboratory, Berkeley, CA 94720, USA

Abstract

We provide a method to correct the observed azimuthal anisotropy in heavy-ion collisions for the event plane resolution in a wide centrality bin. This new procedure is especially useful for rare particles, such as Ω baryons and J/ψ mesons, which are difficult to measure in small intervals of centrality. Based on a Monte Carlo calculation with simulated v_2 and multiplicity, we show that some of the commonly used methods have a bias of up to 15%.

Keywords: Azimuthal anisotropy, flow, event plane

1. Introduction

Azimuthal anisotropy is one of the key observables to study the properties of matter created in high energy heavy-ion collisions (see e.g. [1]). It is characterized by the Fourier decomposition of the azimuthal particle distribution with respect to the reaction plane

$$\frac{dN}{d(\phi - \Psi_{\text{RP}})} = \frac{N_0}{2\pi} \left(1 + 2 \sum_{n=1}^{\infty} v_n \cos[n(\phi - \Psi_{\text{RP}})] \right), \quad (1)$$

where N_0 is the number of particles, v_n is the n -th harmonic coefficient, ϕ is the azimuthal angle of particles and Ψ_{RP} is the azimuthal angle of the true reaction plane which is determined by the beam axis and impact parameter.

One of the standard methods to extract v_n is the *event plane method* [2]. The most important task in this method is to estimate the reaction plane from the measured particles for each harmonic n . We do not distinguish in this paper between reaction plane and participant plane since we discuss only resolution correction. The estimated reaction plane is defined as the *event plane* Ψ_n ($-\pi/n \leq \Psi_n < \pi/n$), but due to the finite multiplicity in nuclear collisions, the event plane can be different from the reaction plane. The observed $v_n^{\text{obs}}(M)$ for a given, small, centrality range M must be corrected by the *event plane resolution* $\mathcal{R}_n(M)$ in order to take into account the difference between true reaction plane and event plane

$$v_n(M) = \frac{\langle \langle \cos[n(\phi - \Psi_m)] \rangle \rangle_M}{\langle \langle \cos[n(\Psi_m - \Psi_{\text{RP}})] \rangle \rangle_M} \equiv \frac{v_n^{\text{obs}}(M)}{\mathcal{R}_n(M)}, \quad (2)$$

where m is the harmonic of the event plane and $n = km$ is the harmonic of interest. Brackets denote the average over events, while double brackets denote the average over particles in all events. Subscript M on the bracket emphasizes that the average is taken for a given centrality M . For simplicity, we will omit (M) from the observables, for example, we will write N_0 instead of $N_0(M)$. In experiment the reaction plane angle Ψ_{RP} in Eq. (2) is not known. Therefore at least two subevent planes are necessary in order to calculate the event plane resolution [2]. An average v_n over a wider centrality range R can be calculated once v_n^{obs} and \mathcal{R}_n are determined within R

$$\frac{\int_R dM N_0 \frac{v_n^{\text{obs}}}{\mathcal{R}_n}}{\int_R dM N_0} \equiv \left\langle \frac{v_n^{\text{obs}}}{\mathcal{R}_n} \right\rangle = \langle v_n \rangle. \quad (3)$$

We introduced brackets $\langle \dots \rangle$ for simplicity, which denote the average over a wide centrality range weighted by particle multiplicity N_0 for a given phase space (e.g. for a given transverse momentum).

\mathcal{R}_n depends on multiplicity and v_n itself, therefore Eq. (3) requires that v_n^{obs} and \mathcal{R}_n are measured in sufficiently small centrality intervals. However, for rare particles (e.g. Ω , J/ψ) it is not always possible to do so. One of the conventional approaches (e.g. see Ref. [3]) is to average v_n^{obs} as well as \mathcal{R}_n separately in a wide centrality range, weighted by the corresponding particle yields, and then take the ratio of $\langle v_n^{\text{obs}} \rangle$ to $\langle \mathcal{R}_n \rangle$. However, this approach systematically overestimates v_n as we will discuss in the Section 3. The main point of this paper is the

following inequality

$$\left\langle \frac{v_n^{\text{obs}}}{\mathcal{R}_n} \right\rangle \neq \frac{\langle v_n^{\text{obs}} \rangle}{\langle \mathcal{R}_n \rangle} \neq \langle v_n^{\text{obs}} \rangle \left\langle \frac{1}{\mathcal{R}_n} \right\rangle \quad (4)$$

where the left hand side is the correct average over a wide centrality bin, while the right hand side shows a commonly used approximation.

We will show the proper way to correct for the finite event plane resolution in wide centrality bins. In Section 2, we derive the equations used to calculate $\langle v_n \rangle$ in our approach. We also show that the derived equations are equivalent to the average calculated from narrow centrality bins (see Eq. (3)). In Section 3, we show a fast Monte Carlo simulation to demonstrate the validity of the method, for the case of v_2 .

2. Implementation

We now show several practical implementations to correct v_n for the event plane resolution in wide centrality bins. There are two or three steps to calculate v_n in wide centrality bins

1. Determine the event plane resolution \mathcal{R}_n as a function of narrow centrality ranges M .
2. Analyse v_n with the weights $1/\mathcal{R}_n$ for any, wide, centrality range of interest.
3. Perform an additional resolution correction (depends on implementation).

In the following two subsections, we discuss detailed implementations how to apply corrections separately for different types of particle identification. For the sake of simplicity, we assume that non-flow effects are negligible, and all correlations between particles are induced by flow. Namely, the azimuthal particle distribution with respect to the event plane can be written as

$$\frac{dN}{d(\phi - \Psi_m)} = \frac{N_0}{2\pi} \left(1 + 2 \sum_n^\infty v_n^{\text{obs}} \cos[n(\phi - \Psi_m)] \right) \quad (5)$$

2.1. Event-by-event particle identification

If the particle of interest can be identified on an event-by-event basis, one can directly calculate $\cos[n(\phi - \Psi_m)]$ for every particle, corrected with the event plane resolution for the corresponding centrality M

$$\frac{\cos[n(\phi - \Psi_m)]}{\mathcal{R}_n}, \quad (6)$$

where \mathcal{R}_n is supposed to be averaged over many events in advance. The event and centrality average of term (6) over $\phi - \Psi_m$ reduces in this case to Eq. (3)

$$\begin{aligned} \langle v_n^{\text{cos}} \rangle &\equiv \frac{\int_R dM \int_0^{2\pi} d(\phi - \Psi_m) \frac{dN}{d(\phi - \Psi_m)} \frac{\cos[n(\phi - \Psi_m)]}{\mathcal{R}_n}}{\int_R dM \int_0^{2\pi} d(\phi - \Psi_m) \frac{dN}{d(\phi - \Psi_m)}} \\ &= \frac{\int_R dM N_0 \frac{v_n^{\text{obs}}}{\mathcal{R}_n}}{\int_R dM N_0} = \langle v_n \rangle \end{aligned} \quad (7)$$

The main difference of our implementation to the conventional approach is the event-by-event \mathcal{R}_n correction in Eq. (7). As we have mentioned earlier, event-by-event \mathcal{R}_n correction does not mean that the \mathcal{R}_n should be calculated event-by-event, but rather the correction is made event-by-event. Practically, the statistical error on the event plane resolution can be ignored if the event plane resolution is good. However, if the event plane resolution is very small then one needs to propagate also the statistical error on the event plane resolution into the final v_n values.

2.2. Statistical particle identification

There are two approaches in case the particle yield of interest can only be extracted statistically: the invariant mass fit method and the event plane method. The invariant mass fit method is almost equivalent to the one introduced in Section 2.1, while the event plane method needs one additional step to obtain the final v_n , which will be discussed below.

2.2.1. Invariant mass fit method

The invariant mass method is quite useful to analyse particles that are detected through their decay products, such as $K_s^0 \rightarrow \pi^+ \pi^-$, $\Lambda \rightarrow p \pi^-$ and so on. The point of this method is to calculate the mean $\cos[n(\phi - \Psi_m)]$ as a function of invariant mass M_{inv}

$$v_n^{S+B}(M_{\text{inv}}) = \langle \cos[n(\phi - \Psi_m)]_{\text{inv}} \rangle, \quad (8)$$

$$\begin{aligned} v_n^{S+B}(M_{\text{inv}}) &= v_n^S \frac{S}{S+B}(M_{\text{inv}}) \\ &\quad + v_n^B(M_{\text{inv}}) \frac{B}{S+B}(M_{\text{inv}}). \end{aligned} \quad (9)$$

where S is the signal yield, B is background yield, v_n^S , v_n^B and v_n^{S+B} are the v_n for signal, background and total particles, respectively. Signal and background contributions are decomposed by taking into account the measured signal-to-background ratio and using a parametrization of the background v_n^B shape [4]. Since the average cosine is calculated in this approach, one can directly extract the v_n^S by subtracting the background contribution. The only modification is to add a weight $1/\mathcal{R}_n$ on an event-by-event basis when one fills the histograms for $\cos[n(\phi - \Psi_m)]$ versus invariant mass similar to the Eq. (7).

2.2.2. Event plane method

The first step in the event plane method is the signal extraction for a given $\phi - \Psi_m$ bin

$$N^{\mathcal{R}}(\phi - \Psi_m) = \int_R dM \frac{1}{\mathcal{R}_n} \frac{dN}{d(\phi - \Psi_m)}, \quad (10)$$

where $N^{\mathcal{R}}(\phi - \Psi_m)$ is the number of particles for a given $\phi - \Psi_m$ bin, weighted for each centrality bin with the inverse of the event plane resolution. The difference to the conventional method is the weight $1/\mathcal{R}_n$ on the particle yields which will properly take into account the centrality dependence of the event plane resolution. Second, one integrates Eq. (10) over $\phi - \Psi_m$ to calculate v_n

$$\begin{aligned} \langle v_n^{\text{obs}, \mathcal{R}} \rangle &\equiv \frac{\int_0^{2\pi} d(\phi - \Psi_m) N^{\mathcal{R}}(\phi - \Psi_m) \cos[n(\phi - \Psi_m)]}{\int_0^{2\pi} d(\phi - \Psi_m) N^{\mathcal{R}}(\phi - \Psi_m)} \\ &= \frac{\int_R dM \int_0^{2\pi} d(\phi - \Psi_m) \frac{dN}{d(\phi - \Psi_m)} \frac{\cos[n(\phi - \Psi_m)]}{\mathcal{R}_n}}{\int_R dM \int_0^{2\pi} d(\phi - \Psi_m) \frac{dN}{d(\phi - \Psi_m)}}. \end{aligned} \quad (11)$$

Note that $v_n^{\text{obs}, \mathcal{R}}$ in Eq. (11) is different from the conventional v_n^{obs} due to the $1/\mathcal{R}_n$ weight on the particle yields. One could immediately notice that the numerator is identical to Eq. (7) with the additional normalization $1/(2\pi \int_R dM N_0)$. The denominator in Eq. (11) is

$$\begin{aligned} &\int_0^{2\pi} d(\phi - \Psi_m) N^{\mathcal{R}}(\phi - \Psi_m) \\ &= 2\pi \int_R dM \frac{N_0}{\mathcal{R}_n} = 2\pi \left(\int_R dM N_0 \right) \left\langle \frac{1}{\mathcal{R}_n} \right\rangle. \end{aligned} \quad (12)$$

Since the normalization factor $2\pi \left(\int_R dM N_0 \right)$ is cancelled out between numerator and denominator, the $\langle v_n \rangle$

is obtained by multiplying $\langle 1/\mathcal{R}_n \rangle$ by the $\langle v_n^{\text{obs}, \mathcal{R}} \rangle$

$$\langle v_n^{\phi-\Psi} \rangle \equiv \langle v_n^{\text{obs}, \mathcal{R}} \rangle \left\langle \frac{1}{\mathcal{R}_n} \right\rangle = \langle v_n \rangle. \quad (13)$$

We would like to emphasize two important points for the event plane method. First, one must take an average of the inverse event plane resolution $1/\mathcal{R}_n$ (not an average of \mathcal{R}_n). Second, the integral $\int_R dM$ in Eq. (11) for both numerator and denominator should be calculated in the same phase space. For instance, if one measures the v_n as a function of transverse momentum p_T , one should calculate $\langle 1/\mathcal{R}_n \rangle$ for each p_T bin.

The new implementation can also be applied for the scalar product method [5, 6] because the scalar product method is a simple extension of event plane method where the magnitude of the Q-vector is considered for both v_n^{obs} and \mathcal{R}_n .

3. Simulation results

In this section we validate our implementation by a fast Monte Carlo simulation for $v_2(p_T)$. As we have mentioned earlier, this approach can be applied for any harmonic of interest.

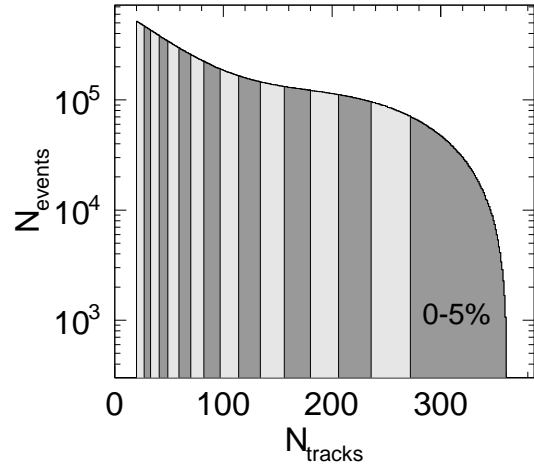


Figure 1: Input multiplicity distribution in the fast Monte Carlo simulation. The shaded area show 0-5%, 5-10%, ..., 75-80% centrality classes.

Figure 1 shows the input multiplicity distribution in 0-80% centrality for the 50 million generated events. The event centrality classes are determined by using the multiplicity distribution as it is typically done in the experimental data. We divide the multiplicity distribution into 16 bins with 5% increments within 0-80%.

For every event a number of tracks according to the input multiplicity distribution was sampled. A Boltzmann like p_T distribution from 0.25–3 GeV/c was used. The input $v_2^{\text{in}}(p_T)$ for every centrality bin was fixed to a parametrization of the following form

$$v_2^{\text{in}}(p_T) = A(1 - e^{-p_T}) \left(\frac{a}{1 + e^{-(p_T-b)/c}} - d \right). \quad (14)$$

The parameter A was increased towards more peripheral centralities. Furthermore we have added for every event a Gaussian smearing on v_2^{in} with a width of 0.05. Figure 2 depicts the used $v_2^{\text{in}}(p_T)$ for the 16 centrality bins. The event Q-vector was calculated according to Ref. [2].

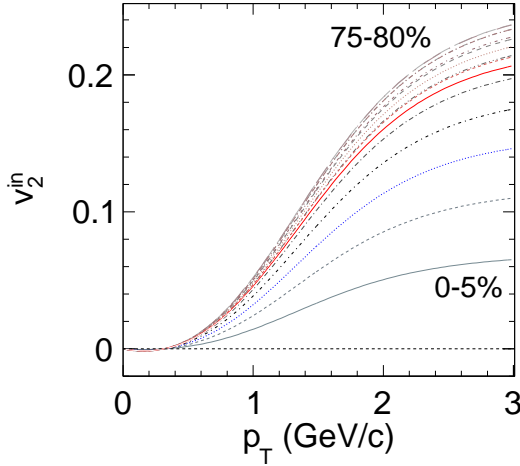


Figure 2: (Color online) Input $v_2(p_T)$ distributions for different centralities. Each line corresponds to a 5% centrality range. $v_2^{\text{in}}(p_T)$ increases towards more peripheral events. The applied Gaussian smearing is not shown.

Figure 3 shows the random subevent plane resolution as a function of centrality. For each event, particles are randomly divided into two different groups in order to evaluate the resolution \mathcal{R}_2 . The result shown here is the subevent plane resolution by using Eq. (14) in Ref. [2]. The resolution reaches a maximum of 0.45 around 30% centrality, it decreases towards more central and peripheral events because of a lower v_2 in central and less multiplicity in peripheral events.

Figure 4 shows an example of a particle azimuthal distribution with respect to the second harmonic event plane in a narrow p_T bin. The particle yields are weighted by the inverse event plane resolution as indicated by $N^{\mathcal{R}}$ in the y-axis title. The dashed line represents

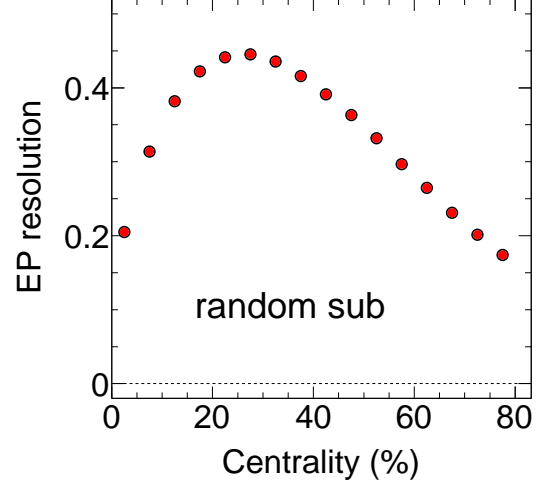


Figure 3: (Color online) Random subevent plane resolution for the second harmonic plane as a function of centrality. The resolution is calculated from random subevents.

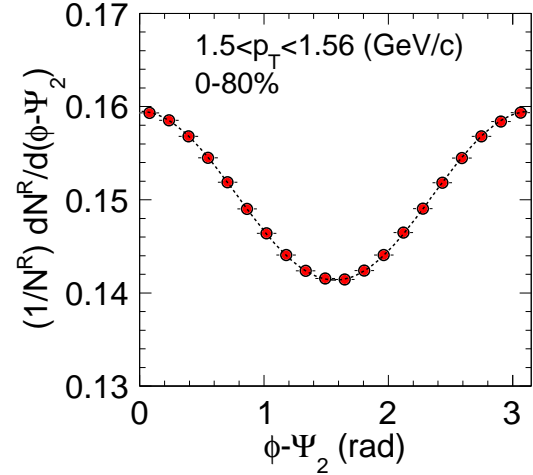


Figure 4: (Color online) Azimuthal distribution of particles with respect to the second harmonic event plane at $1.5 < p_T < 1.56$ GeV/c in 0–80% centrality bin. The dashed line is the fit result for $1 + 2v_2^{\text{obs}} \cos[2\phi - 2\Psi_2]$.

resents a fit with $1 + 2v_2^{\text{obs}, \mathcal{R}} \cos[2\phi - 2\Psi_2]$. The yield extraction and fit are repeated for all other p_T bins.

Figure 5 shows $\langle v_2 \rangle$ as a function of p_T in the 0-80% centrality bin. For comparison, we also plot the observed $\langle v_2^{\text{obs}} \rangle$ without resolution correction as shown by solid grey circles. The difference between observed and corrected $\langle v_2 \rangle$ gives the size of the resolution correction. The input $\langle v_2^{\text{in}} \rangle$ of the simulation is shown as a magenta solid line. We tested both, the direct cosine calculation $\langle v_2^{\text{cos}} \rangle$ from Eq. (7) and the event plane method $\langle v_2^{\phi-\Psi} \rangle$ from Eq. (13), as shown by open blue stars and solid blue stars, respectively in panel (a) and (b). One can see that both direct cosine and event plane methods are consistent with the input $\langle v_2^{\text{in}} \rangle$. The data points are in agreement with 0 within 0.3%. Panel (b) shows the observed $\langle v_2^{\text{obs}} \rangle$, corrected by the inverse mean event plane resolution $\langle \mathcal{R} \rangle^{-1}$ (green line) and the mean inverse event plane resolution $\langle \mathcal{R}^{-1} \rangle$ (red line). In panel (c) we show a correction similar to panel (b) but with the event plane resolution calculated for every single p_T bin. The relative difference $\Delta \langle v_2 \rangle$ of the corrected $\langle v_2 \rangle$ values to the input $\langle v_2^{\text{in}} \rangle$ is shown in the lower panels. For the correction with $\langle \mathcal{R} \rangle^{-1}$ and $\langle \mathcal{R}^{-1} \rangle$ we get a $\Delta \langle v_2 \rangle / \langle v_2^{\text{in}} \rangle$ of 5% and 15%, respectively. The difference becomes smaller if the average resolution is calculated for every p_T bin as shown in panel (c), but we still obtain relative deviations of 4.5% ($\langle \mathcal{R} \rangle_{p_T}^{-1}$) and 10% ($\langle \mathcal{R}^{-1} \rangle_{p_T}$). In all cases the relative difference is almost independent of p_T .

4. Summary

We have introduced an implementation to avoid event plane resolution effects of wide centrality bins on the v_n measurements. The new approach is essentially an extension of existing event plane methods. The basic modification is to add an inverse of event plane resolution weight to the cosine term or to the particle yields depending on the method. We confirmed that our approach reproduces the input $\langle v_2^{\text{in}} \rangle(p_T)$ in a wide centrality bin, whereas the conventional corrections lead to a bias as large as $\sim 15\%$ on the reconstructed $\langle v_2 \rangle$ with our fast Monte Carlo simulation.

Acknowledgements

We thank Arthur Poskanzer and Shusu Shi for discussions. We also thank Arthur Poskanzer for comments on the manuscript. This paper was funded in part by the US Department of Energy under Contract No. DE-AC03-76SF00098.

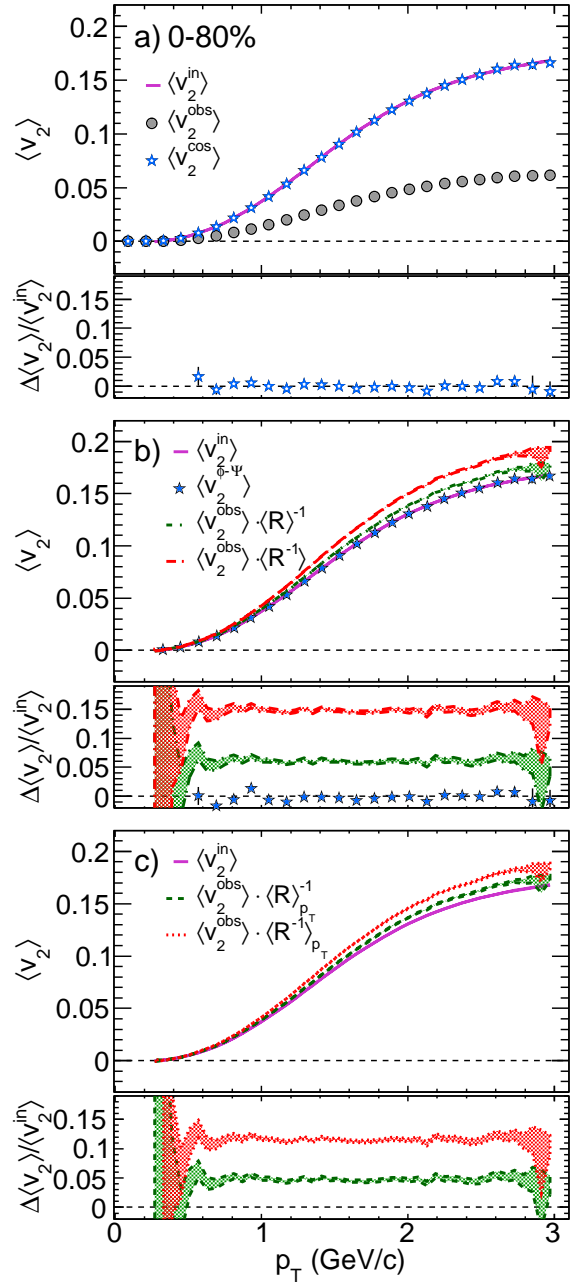


Figure 5: (Color online) Results of v_2 as a function of p_T with different approaches of resolution corrections. The magenta solid line corresponds to the input $\langle v_2 \rangle$, gray filled circles are the observed $\langle v_2^{\text{obs}} \rangle$ without resolution correction, blue open stars in panel (a) are from the direct cosine calculation from Eq. (7), blue filled stars in panel (b) are from the event plane method from Eq. (13). Other lines show the observed $\langle v_2^{\text{obs}} \rangle$ with different mean event plane resolution corrections. In panel (c) the event plane resolution is calculated for every p_T bin separately.

References

- [1] S. A. Voloshin, A. M. Poskanzer and R. Snellings, arXiv:0809.2949 [nucl-ex].
- [2] A. M. Poskanzer and S. A. Voloshin, Phys. Rev. C **58**, 1671 (1998) [nucl-ex/9805001].
- [3] M. M. Aggarwal *et al.* [STAR Collaboration], Phys. Rev. C **84**, 034909 (2011) [arXiv:1006.1961 [nucl-ex]].
- [4] N. Borghini and J. Y. Ollitrault, Phys. Rev. C **70**, 064905 (2004) [nucl-th/0407041].
- [5] C. Adler *et al.* [STAR Collaboration], Phys. Rev. C **66**, 034904 (2002) [nucl-ex/0206001].
- [6] M. Luzum and J. -Y. Ollitrault, arXiv:1209.2323 [nucl-ex].